N65 29293

NASA CR-54452

SECOND QUARTERLY REPORT
ON
DEVELOPMENT OF OPTICAL COATINGS
FOR
CdS THIN FILM SOLAR CELLS

By

J. C. Schaefer, E. R. Hill

Prepared For

NATIONAL AERONAUTICS AND SPACE ADMINISTRATION

CONTRACT NAS3-6464

THE HARSHAW CHEMICAL CO.

NOTICE

Requests for copies of this report should be referred to:

National Aeronautics and Space Administration
Office of Scientific and Technical Information
Attention: AFSS-A
Washington, D.C. 20546

NASA CR-54452

SECOND QUARTERLY REPORT

DEVELOPMENT OF OPTICAL COATINGS FOR CdS THIN FILM SOLAR CELLS

by

J. C. Schaefer, E. R. Hill

Prepared For

NATIONAL AERONAUTICS AND SPACE ADMINISTRATION

CONTRACT NAS3-6464

SECOND QUARTERLY REPORT

DEVELOPMENT OF OPTICAL COATINGS FOR CdS THIN FILM SOLAR CELLS

by

J.C. Schaefer, E.R. Hill

Prepared For

NATIONAL AERONAUTICS AND SPACE ADMINISTRATION

March 1, 1965 to June 1, 1965

Contract NAS 3-6464

Technical Management
NASA Lewis Research Center
Cleveland, Ohio
Space Power Systems Division
Clifford Swartz

Harshaw Chemical Company
Crystal-Solid State Division
1945 E. 97th Street
Cleveland 6, Ohio

FOREWORD

This report was prepared by The Harshaw Chemical Company, Crystal-Solid State Division under Contract NAS 3-6464 for the NASA Lewis Research Center. Dr. A. E. Potter and Mr. C. Swartz have served as Technical Advisor and Project Manager respectively.

The Harshaw Solid State Laboratory is directed by Dr. J. M. McKenzie, Technical Director. Project direction is provided by Mr. E. R. Hill with Mr. J. C. Schaefer serving as Project Supervisor. The following Harshaw Chemical Company personnel have contributed to this program: R. W. Olmsted, R. J. Humrick and A. Hartzler.

TABLE OF CONTENTS

LIST OF FIGURES

DEVELOPMENT OF OPTICAL COATINGS
FOR
CdS THIN FILM SOLAR CELLS

By J. C. Schaefer and E. R. Hill

SUMMARY

The apparatus for RF sputtering of dielectrics is operational and films of glass have been deposited. Reflectance measurements indicate films in the range of 4 microns thickness to show the desired infrared reflectance characteristic. Work is underway to improve the deposited film thickness uniformity and increase the deposition rate.

Oxygen is being added to the sputtering gas to reduce the stresses in the deposited films.

INTRODUCTION

The purpose of this program is to develop and apply optical coatings to CdS solar cells for the purpose of increasing the power conversion efficiency. It is desired to maximize the amount of light entering the cell in the region of the spectrum where the cell is sensitive, reject all others, and reduce the operating temperature of the cell in outer space. These conditions are not all independent since a coating which reflects strongly in the infrared will also reduce the emissivity in the region of maximum cell reradiation. The objectives stated can be reached by developing a coating with a high transmission to wave lengths less than about 1 micron, has a refractive index of about 1.2 to 1.3 in this same range and absorbs relatively strongly (about 10^{-3} to 10^{-4} cm^{-1}) in the range of 5 to 30 microns. These properties are satisfied by ordinary glass and consequently has been the first material to be investigated to any extent.

Other obvious properties to be desired are compatibility with the device, mechanical and chemical stability, and resistance to environmental effects. Additional, it is desirable to have the coating seal the cell from atmospheric water vapor.

During the second quarter of the program a coating of SiO_x possessing the desired optical properties has been produced. Samples have been shipped to the NASA, Lewis Research Center. Evaluation of the other properties remain.

RF SPUTTERING APPARATUS

The dielectric sputtering equipment is operating quite satisfactorily at essentially the design conditions for the system. These are:

Ambient Pressure	5×10^{-4} Torr
Target to substrate spacing	6 cm
Power to target	400 watts
Target sputtering rate	2×10^{-4} cm/hour
Target material	Pyrex

Under these conditions films are being made for the determination of optical and mechanical properties of the deposited glass films. With these same conditions, any dielectric which can be prepared in the form of a thin sheet can be used as the target and sputtered at essentially the same rate. This method for the formation or deposition of films offers distinct advantages over thermal evaporation, particularly for the exploratory stages. For instance, dielectrics such as glass are very difficult to evaporate since the molten glass reacts with available crucible materials. Techniques such as electron beam melting can also be used, but crucible attack is a problem. Thus, for thermal evaporation of different dielectrics, the equipment must be altered for each material. In sputtering, only the target material is changed. For this phase of the program, then, sputtering is much more flexible.

A few engineering difficulties have been encountered in making the sputtering system operational. From the description of operation given in the first quarterly report, it will be recalled that the two major requirements are a means of producing a plasma at low gas pressures and a means of accelerating the positive gas ions toward the dielectric target. A schematic diagram of the equipment is shown in Figure 1.

The elements for sputtering are contained in an 18 x 30 inch bell jar where the gas pressure is maintained at about 10^{-3} Torr. A field applied between the thermionically emitting cathode and the cold anode produces a plasma column. This is constricted by the magnetic field to a current density of about 0.1 amps/cm^2. The r - f generator is connected to the target and cathode. The plasma column is essentially field free, since the potential difference between anode and cathode during operation is only 75 volts. The r - f generator is then coupled to the target through the plasma column. On the half cycle with the target negative with respect to the cathode, positive gas ions accelerate toward the target, sputtering material when they strike. Since the target is an insulator, a positive charge builds up on the target surface, reducing the accelerating field. On the positive half cycle, electrons from the plasma discharge the target, and charge is somewhat negatively. Thus, it is clear that the impedance seen by the r - f generator is non-linear due to the charging of the insulator and also non-symmetrical due to the different mobilities of the positive gas ions and electrons in the plasma. This makes the impedance matching of the generator to its load extremely difficult to analyze and necessitates a certain amount of trial and adjustment. Most of the difficulties with the system were centered about this area and considerable effort was spent in working out the coupling network. Our experiments have led to a tapped π network shown in Figure 2 which is relatively flexible and easily adjusted.

DEPOSITION PARAMETERS

Film deposition rate is a formation of the rate of material sputtering, gas pressure, and source - substrate geometry. The rate at which material is removed from the target depends on the current and energies of the bombarding gas ions, (electrons produce a negligible contribution). The yield of sputtered atoms per incident ion is linear with energy above a threshold energy which is typically 100 ev. Consequently, for target potentials larger than 100 volts, the sputtering rate is proportional to the power dissipated at the target.

The sputtered atoms are scattered by the gas in the bell jar; this is expressed analytically as

$$N(x) = N_o e^{-\frac{X}{L}}$$

N = number of particles at a distance x from the source

N_o= number of particles leaving the surface of the source

X = distance from the source

L = mean free path of the particle in the gas

L = 5 cm at a pressure of 10^{-3} Torr

Assuming a scattered particle does not deposit on the substrate, this says that at a spacing of 5 cm between the substrate and target, about 37% of the sputtered particles reach the substrate with a bell jar pressure of 10^{-3} Torr. At 5×10^{-4} Torr, 61% reaches the substrate. Consequently, it is necessary to operate at low pressures to achieve high deposition rates. This is one of the functions of the magnetic field in that it causes the electrons to describe helical paths as they move toward the anode, increasing the probability of a collision with a gas atom. This allows the gas pressure to be decreased. The spacing of 6 cm and a pressure of 5×10^{-4} Torr has been found to be satisfactory.

Finally, the target-substrate geometry affects the overall collection of the sputtered material and the variation of deposited film thickness. The sputtered material leaves the target describing the Lambert cosine law distribution. Thus the fraction of the total sputtered material which is deposited is equal to the solid angle which the substrate subtends at the target. This immediately implies that the deposited film will be uniform in thickness only for special geometries. For a 7 cm x 7 cm square, (with no scattering) this arrangement is 4 point sources at the corners of a 7 cm square each 7 cm perpendicular distance from the substrate. This obviously gives a 25% collection efficiency, but also produces a thickness variation less than 10%. Compromises can be made with area sources closer to the substrate and closer together. This geometry has a further advantage in that the impedance of the target seen by the generator is increased and the peak target potential increased. This increases the sputtering efficiency since more of the average power at the target is dissipated at voltages above the sputtering threshold.

MEASUREMENTS

1. Sputtering and deposition rate

Sputtering rate has been measured by weighing the target before and after sputtering. By this method it has been determined that 400 watts are dissipated over a 4 inch diameter glass disc producing a removal rate of about 2 microns per hour. Over the surface of a 7 cm square cell, 6 cm from the disc, the average deposition rate was about 0.3 to 0.4 microns per hour. A variation of about 50% in film thickness was found over the substrate surface. The target geometry of 4 sources will improve both these figures.

2. Reflectance

As noted in the first quarterly report, the optical property of interest is the total infrared reflectance. The surface of the CdS cell is quite diffuse and so a considerable portion of the reflected light is scattered. The equipment available measures specular reflectance, therefore measurements must be compensated to find the total reflectance. To accomplish this, the sample to be measured is divided into four sections. The first quarter is untreated, the second is coated with an opaque layer of aluminum, the third quarter is coated with glass only, while the fourth quarter is coated with both the layer of glass and the opaque layer of aluminum. Assuming the aluminum to be totally reflecting, we can compare the specular reflectances from these surfaces to find the total reflectance of the glass surface. Figure 3 shows the specular reflectance of a typical cell coated as above. The interference pattern of the CdS on molybdenum is seen along with the evidence for Rayleigh scattering. The CdS film thickness can be calculated from the relation.

$$\text{Thickness} = \frac{N}{2(u^2 - \sin^2 I)^{\frac{1}{2}}(V_1 - v_2)}$$

N = number of maxima between v_1 and v_2

u = refractive index

I = incidence angle = 13°

v_1 and v_2 = wave numbers of extreme maxima in cm^{-1}

$$\text{Thickness} = \frac{21}{2(2.5^2 - .22^2)^{\frac{1}{2}}(2000-600)}$$

$$= 30 \text{ microns}$$

Figure 4 is the reflectance spectrum of the CdS cell with an opaque aluminum overlay. This curve demonstrates that Rayleigh scattering is very important and that the average particle size of the surface being coated is of the order of 10 microns. The particles have a distribution of sizes since the reflectance does not follow the ν^{-4} dependence, but is a more slowly varying function. Figure 5 is the reflectance spectrum for the portion of the cell coated first with 4.3 microns of glass and then an opaque layer of aluminum. The character of the surface is essentially unchanged by the layer of glass, except that it is slightly more diffusely reflecting. Figure 6 is the reflectance spectrum of the cell coated with 4.3 microns of glass. First, the interference pattern due to the CdS film is again in evidence. Since the amplitude of the variation in the interference pattern decreases toward shorter wavelengths, Rayleigh scattering is also present. More important, however, is the lack of the interference pattern in the ranges from 7 to 11 microns and 17 to 30 microns. This indicates the absorption bands of the glass layer are reducing the reflectance of the surface and also are absorbing the light before it can be reflected from the CdS and molybdenum. This is exactly the behavior required. The next step is to deposit a layer about 10 microns thick to determine whether the absorption bands will widen or further reduce the reflectance. Samples described above have been forwarded to the NASA, Lewis Research Center.

Figures 7, 8, and 9 show the characteristics of thinner glass coatings on the cell. Figure 7 shows the reflectance of the coated cell with the aluminum overlay. Figure 8 is the reflectance spectrum of the bare CdS cell, showing the interference pattern of the 30 microns thick CdS + barrier film. Comparing Figures 7 and 8, it is seen that the maxima of the interference pattern correspond to total reflection of the incident beam and that the minima are greater than zero. This implies that the molybdenum is totally reflecting, the front surface of the cell is approximately 30% reflecting and the cell is transparent to this region of the infrared. Figure 9 is the reflectance spectrum of the cell coated with about 1 micron of glass. Clearly the reflectance is reduced and the absorption bands in the 10 micron region are beginning to appear. However, the glass is too thin to give the desired reduction in reflectance.

3. Film Stress

It has been observed that the glass films deposited on the CdS thin film cell are under stress. This stress is sometimes high enough to cause peeling in the thicker films. Workers in this field have found the stress to be related to the composition of the ambient gas used in sputtering. The addition of oxygen reduces the stress, and has been reported to cause a reversal in sign as the oxygen concentration increases. Experiments are being conducted with oxygen being added to the sputtering gas to improve film adhesion.

WORK PLANNED FOR NEXT QUARTER

Thicker coatings (10 microns) will be deposited to extend the reflectance data.

Oxygen will be added to the sputtering gas to reduce film stresses.

Humidity testing of cells with coatings will be started.

Four source geometry will be used to improve film thickness uniformity.

Representative samples will be forwarded periodically.

Preliminary experiments involving additional coating materials will be initiated.

FINANCIAL SECTION

Contract NAS 3-6464

Professional	Manhours
J. C. Schaefer	126
E. R. Hill	179
R. W. Olmsted	479
R. J. Humrick	420
A. Hartzler	464
Total	1668

Non- Professional	
Total	75

Total Contract	$75,003.00
Funds for Cost	70,853.00
Funds Expended	41,539.00
Funds remaining	$29,314.00

TABLE I

SPUTTERING DATA

Date	Ion Gauge (μHg)	Anode Potential (Volts)	Anode Current (Amp.)	Net RF Power (Watts)	Magnet Current (Amps)	Target to Substrate (cm)	Substrate Temperature (^{o}C)	Target Removal Rate (μ/hr.)	Deposition Rate (μ/hr.)	Remark
4-8	10.0			200					.02	1-3/4" RF PROBE - Aryon Gas
4-12	3.0			130		8.3			.1	
4-13	3.0			175		8.3		1.25	.015	"
4-21	0.5	90	2.0	320	5.0	6.0			.24	4" RF PROBE Aryon Gas
4-22	0.65	88	1.3	320	5.0	6.0			.5	"
4-23	0.5	85	1.4	330	5.0	8.6			.38	"
4-27 to 4-30	0.65	81	1.75	317	4.7	6.4			.51	"
5-17 to 5-18	0.52	76	2.0	335	4.6	6.0			.25	"
5-19 to 5-21	0.53	78	1.7	340	4.4	6.0	300		.25	"
5-25	0.50			400	4.4	6.0	233		.27	"
5-26	0.55	87	1.7	390	4.4	6.0	208		.27	"
5-27 to 5-28	0.55	85	1.5	320	4.4	6.0	234	1.95	.36	"
6-3 to 6-4	0.54	85	1.6	355	4.4	6.6	200	2.06	.26	"
6-7	0.54	90	.5	340	4.4	6.0	232		.13	4" RF PROBE Ar-Air Mixture

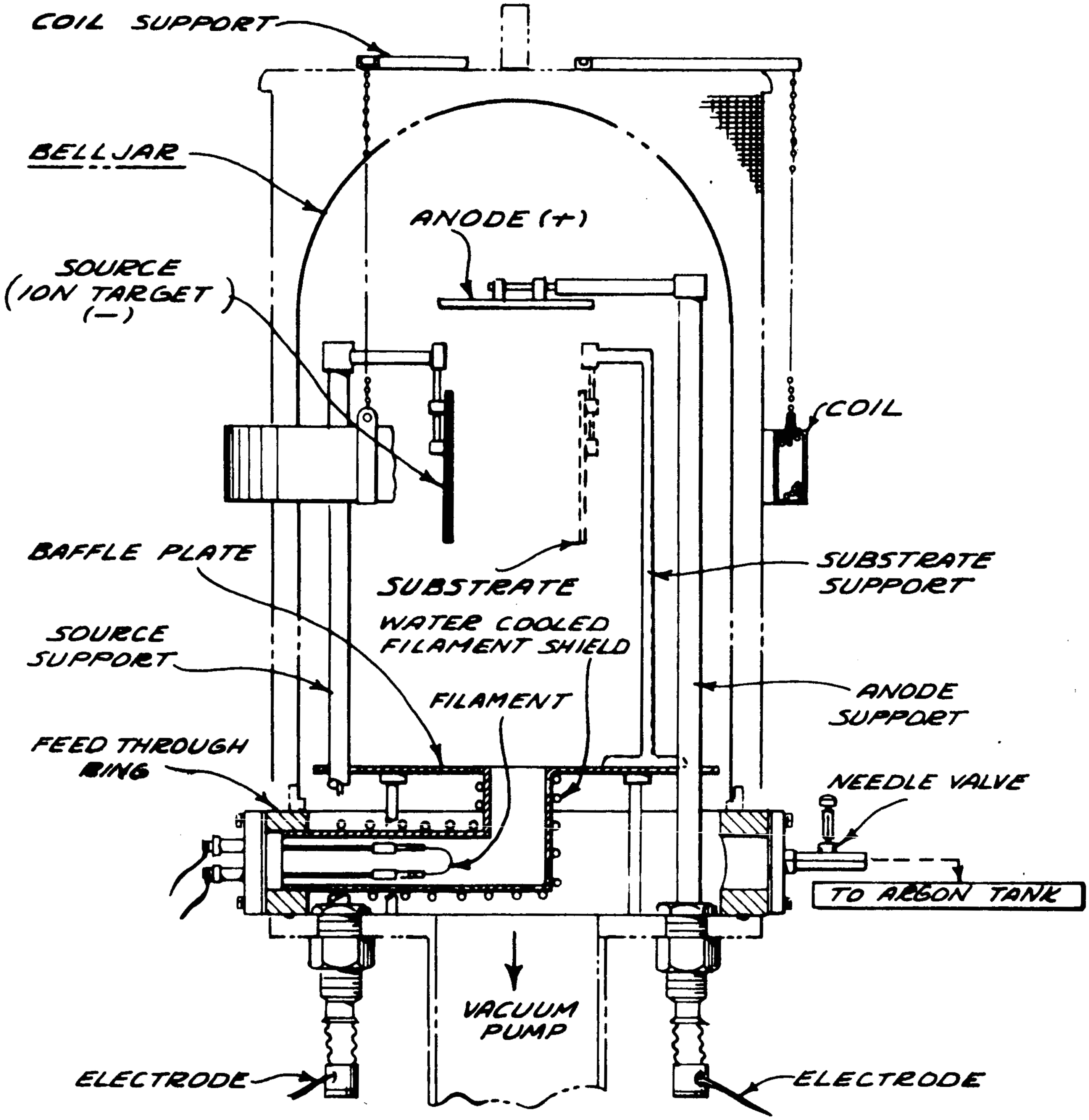

SCHEMATIC DIAGRAM OF SPUTTERING APPARATUS SHOWING CHAMBER COMPONENTS

FIG. 1

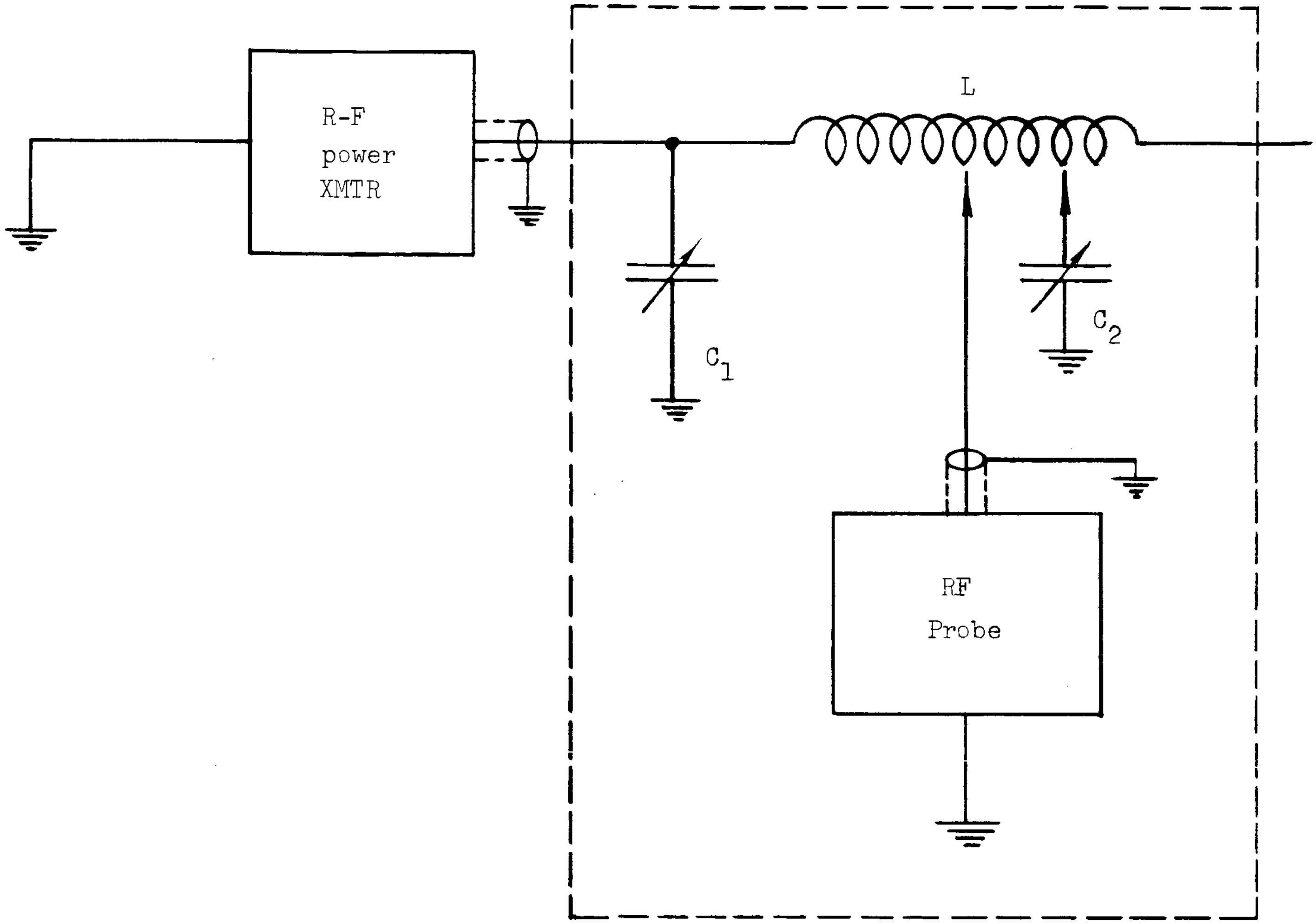

Figure 2

"TAPPED-π" IMPEDANCE MATCHING NETWORK

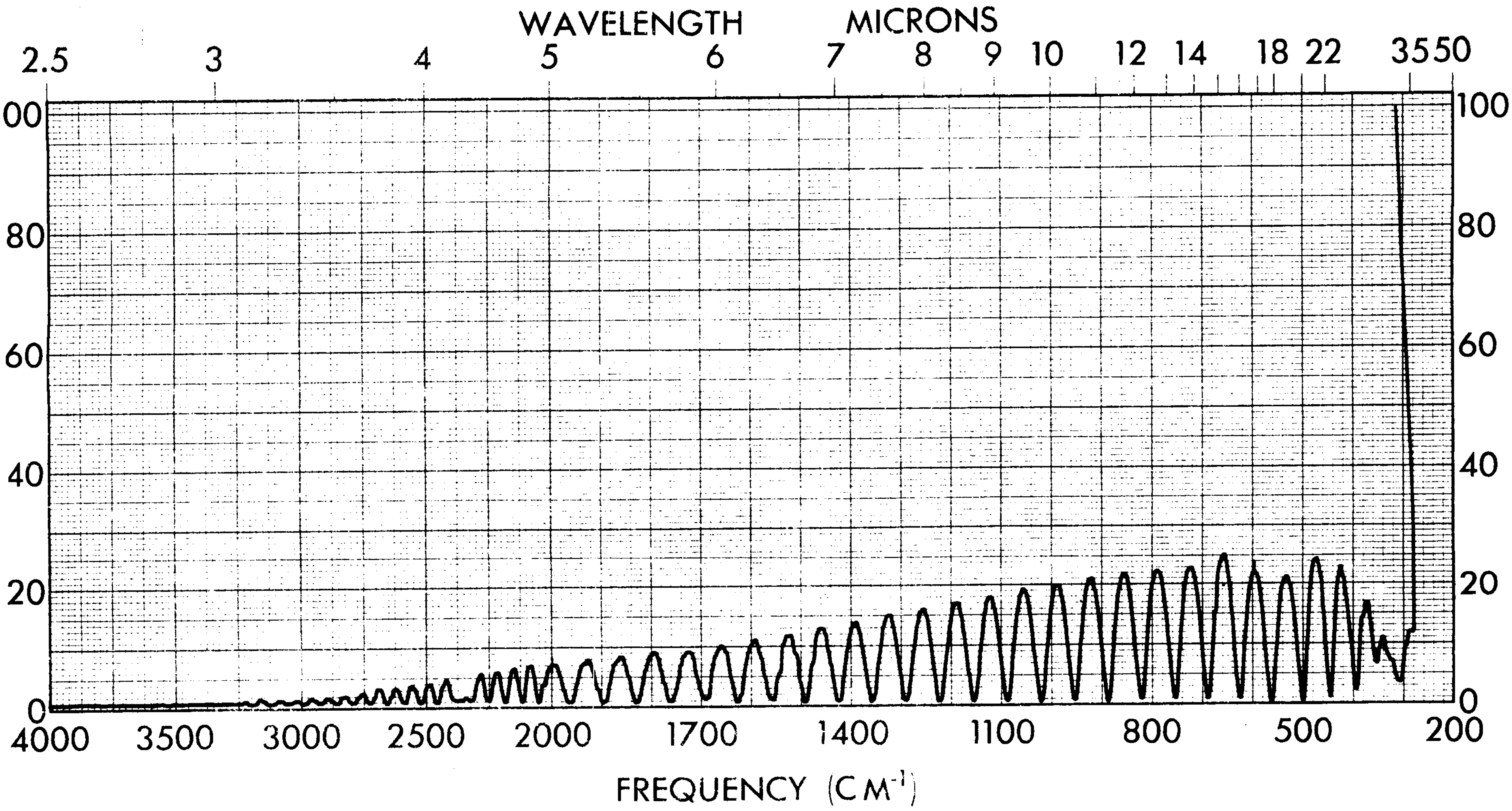

Spectrum No. G-1489

Sample: CdS Cell

Origin: AN 64198

Phase: Solid

Date: 6-7-65

Remarks: Specular Reflectance Spectrum

Figure 3. Reflectance of CdS Cell No. M526

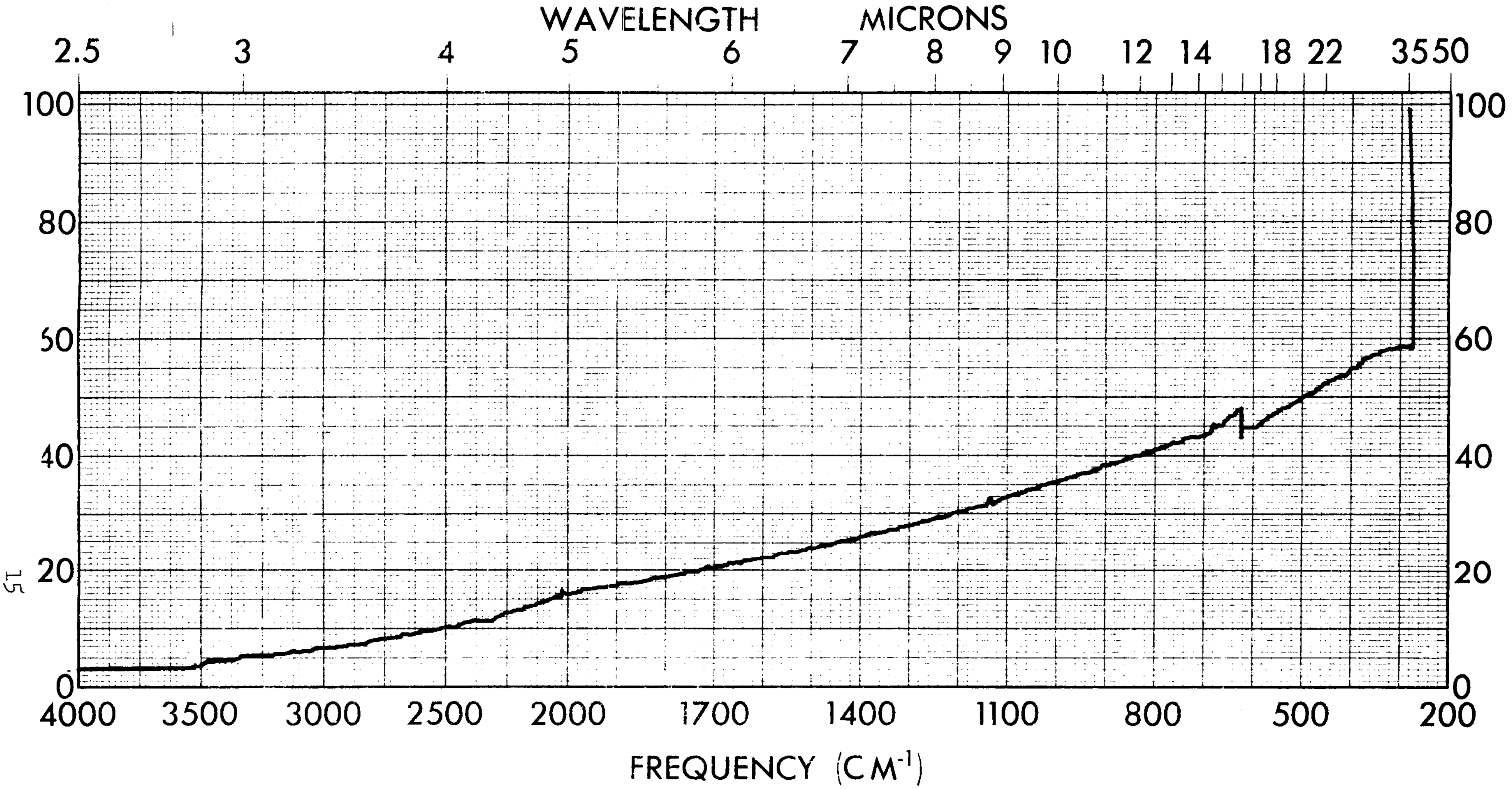

Spectrum No. G-1487

Sample: Al on CdS Cell

Origin: AN 64198

Phase: Solid

Date: 6-7-65

Remarks: Specular Reflectance Spectrum

Figure 4. Reflectance of Aluminum on CdS Cell No. M526

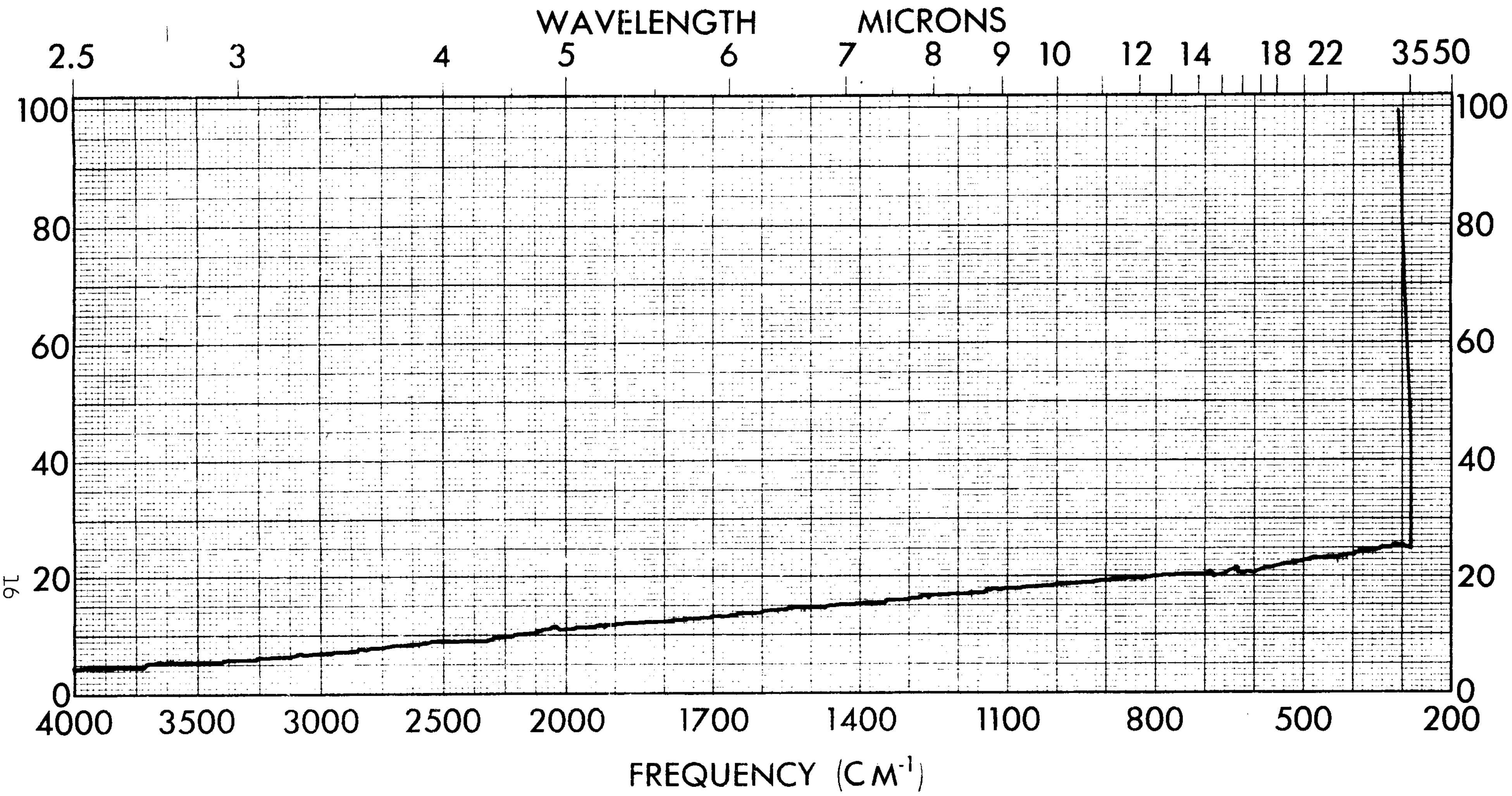

Spectrum No. G-1488

Sample: SiO$_x$ over Al on CdS Cell

Origin: AN 64198

Phase: Solid

Date: 6-7-65

Remarks: Specular Reflectance Spectrum

Figure 5. Reflectance of SiO$_x$ on Al over CdS No. M526

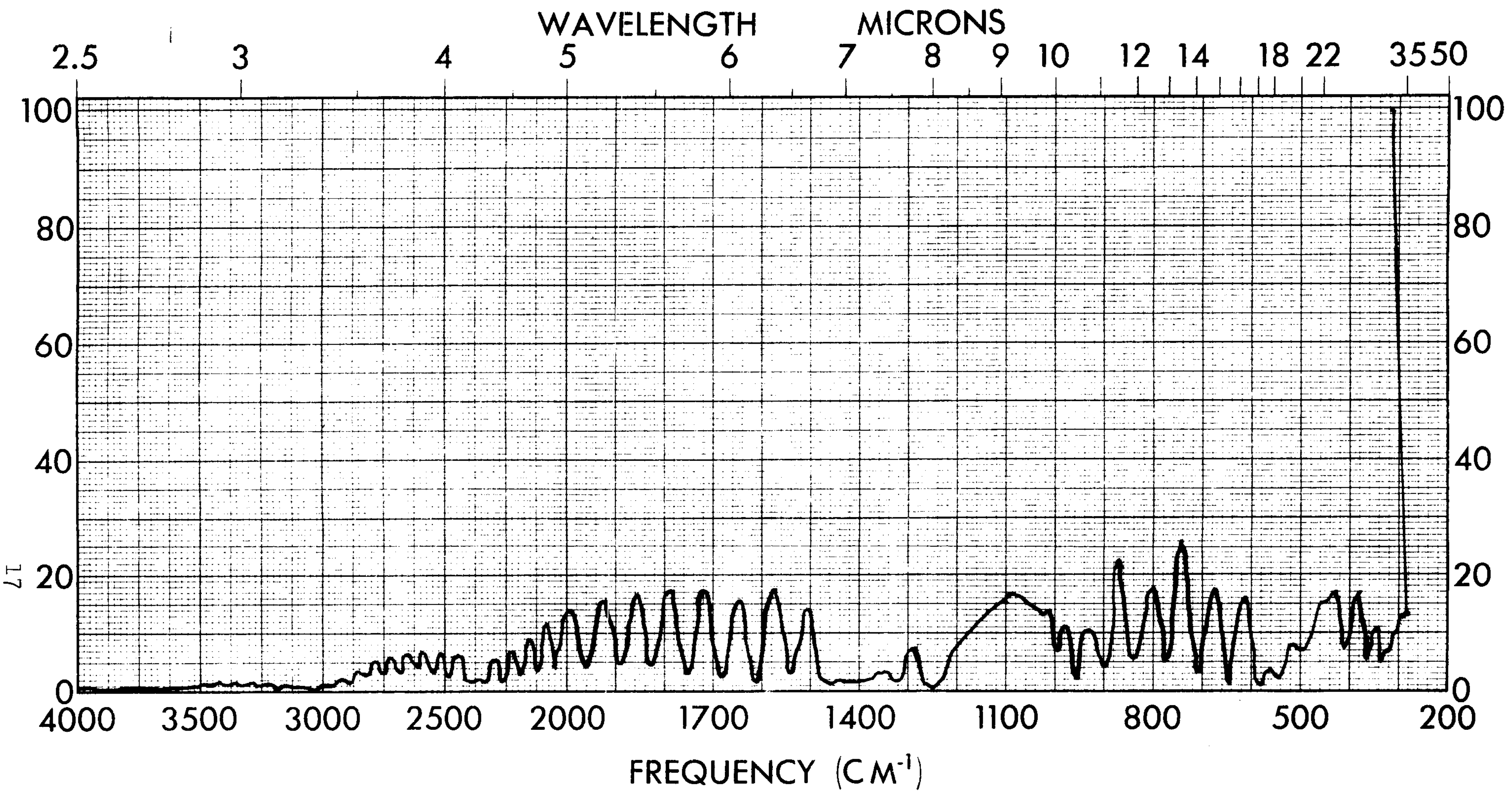

Spectrum No. G-1490

Sample: SiO_x on CdS Cell

Origin: AN 64198

Coating Thickness: 4.3 microns

Phase: Solid

Date: 6-7-65

Remarks: Specular Reflectance Spectrum

Figure 6. Reflectance of SiO_x on CdS Cell No. M526

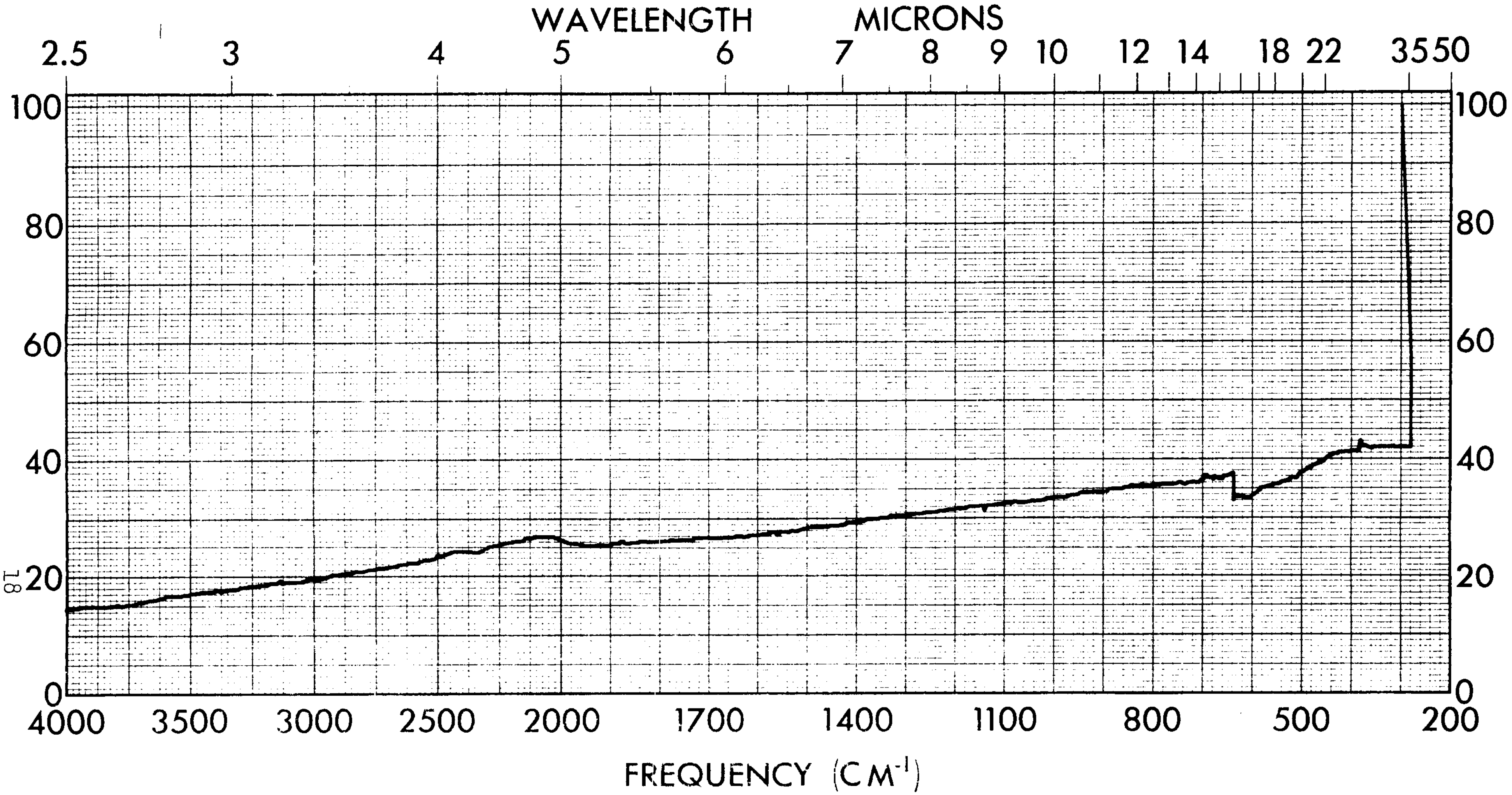

Spectrum No. G-1484

Sample: SiO_x over Al on CdS

Origin: AN 64198

Phase: Solid

Date: 6-7-65

Remarks: Specular Reflectance Spectrum

Figure 7. Reflectance of SiO_x on Al over CdS Cell No. Z159C

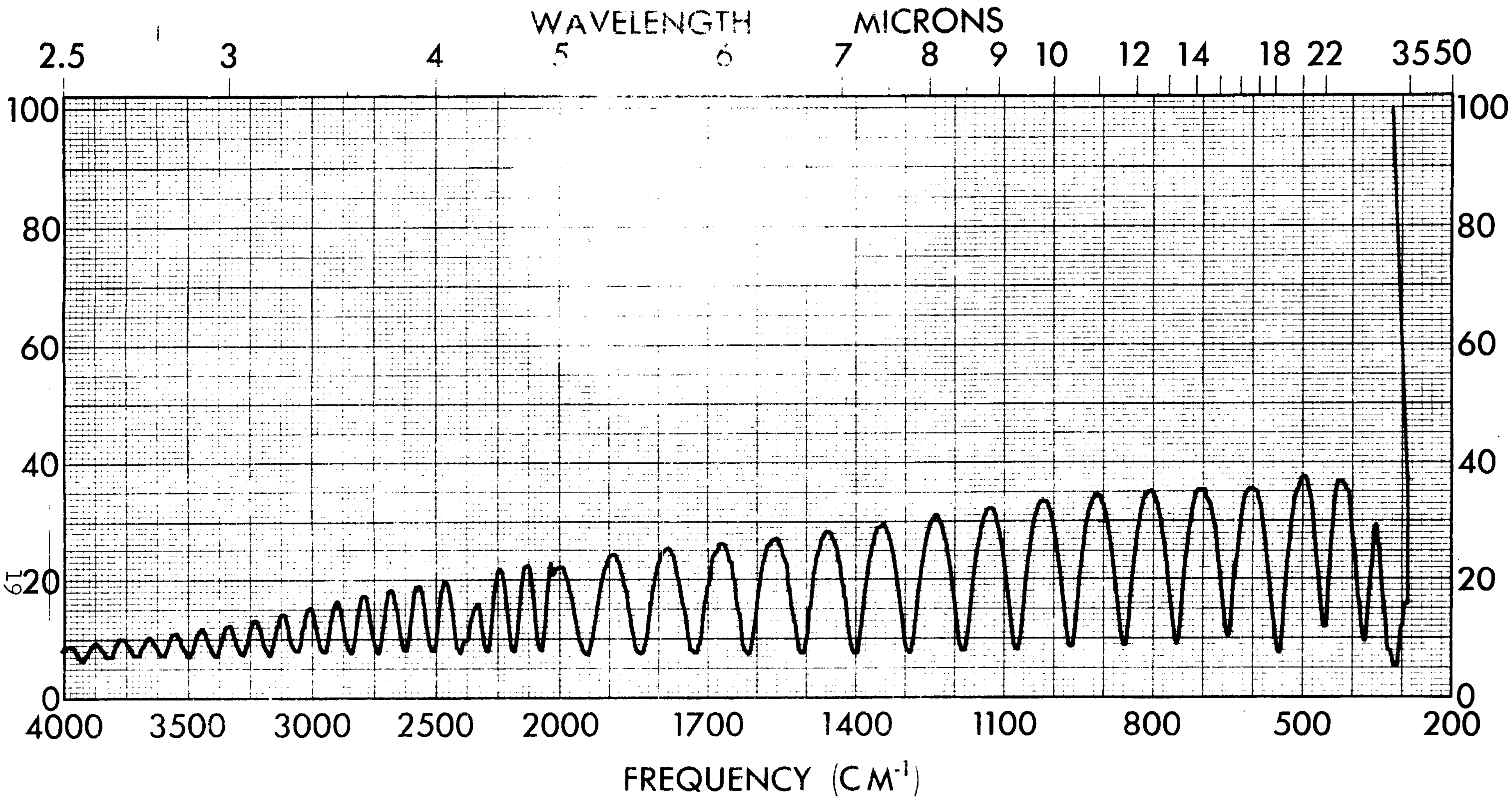

Spectrum No. G-1485

Sample: CdS Cell

Origin: AN 64198

Phase: Solid

Date: 6-7-65

Remarks: Specular Reflectance Spectrum

Figure 8. Reflectance of CdS Cell No. Z159C

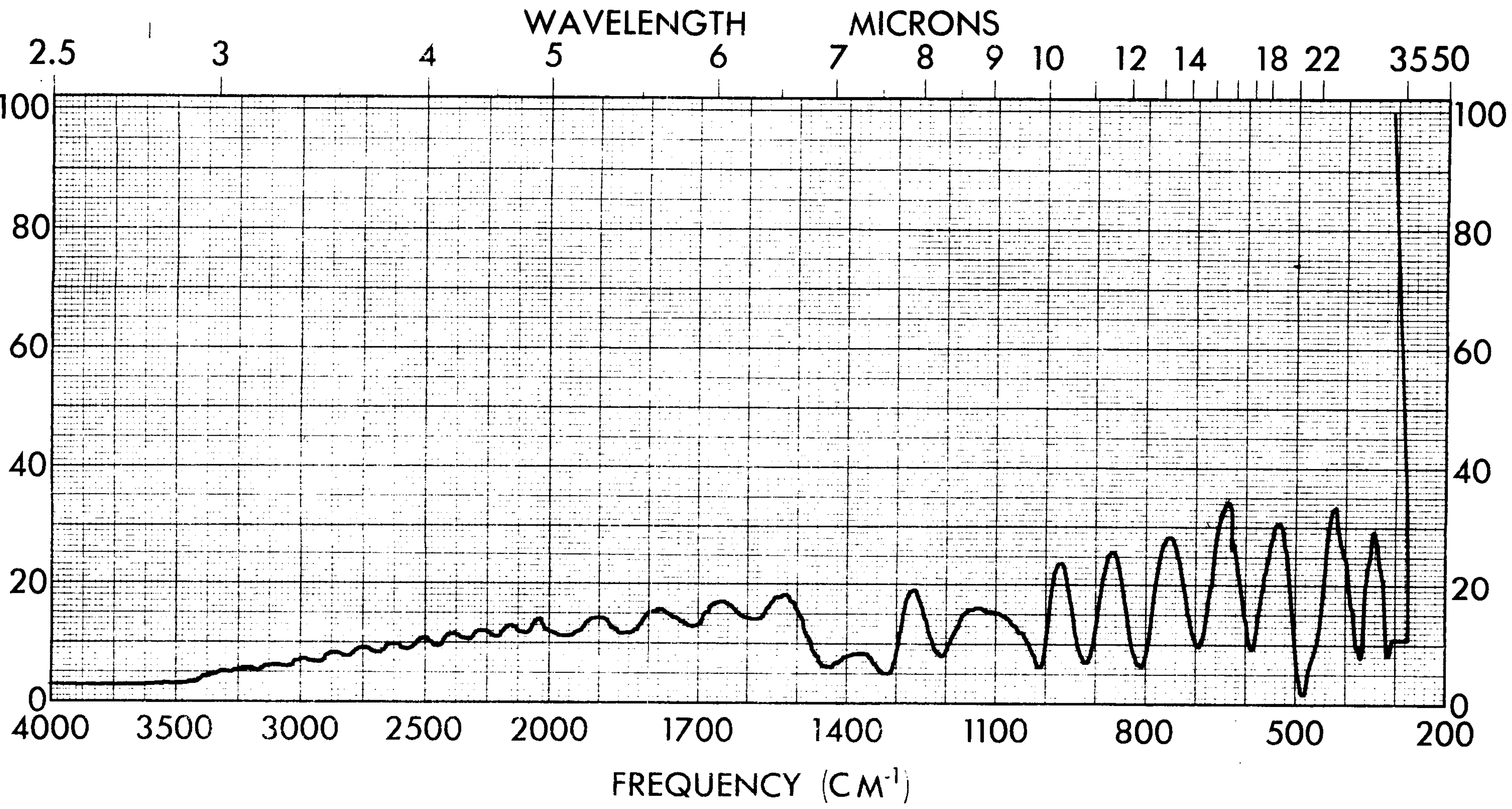

Spectrum No. G-1486

Sample: SiO_x on CdS Cell

Origin: AN 64198

Coating Thickness: 1.16 microns

Phase: Solid

Date: 6-7-65

Remarks: Specular Reflectance Spectrum

Figure 9. Reflectance of SiO_x on CdS Cell No. Z159C

Harshaw Chemical Company
Contract NAS3-6464

Quarterly Reports

DISTRIBUTION LIST

	No. of Copies
National Aeronautics and Space Administration	
Washington, D. C. 20546	
Attention: Arvin H. Smith/RNW	2
National Aeronautics and Space Administration	
Washington, D. C. 20546	
Attention: H. B. Finger/RP	1
National Aeronautics and Space Administration	
Washington, D. C. 20546	
Attention: Millie Ruda/AFSS-LD	1
National Aeronautics and Space Administration	
Scientific and Technical Information Facility	
P. O. Box 5700	
Bethesda, Maryland 20546	
Attention: NASA Representative	5 + 1 repro.
National Aeronautics and Space Administration	
Goddard Space Flight Center	
Greenbelt, Maryland 20771	
Attention: W. R. Cherry	1
Attention: M. Schach	1
Attention: B. Mermelstein, Code 672	1
Attention: J. W. Callaghan, Code 621	1
Attention: Librarian	1
Attention: P. H. Fang, Code 633	5
National Aeronautics and Space Administration	
Lewis Research Center	
21000 Brookpark Road	
Cleveland, Ohio 44135	
Attention: John E. Dilley, MS 500-309	1
Attention: B. Lubarsky, MS 500-201	1
Attention: H. Shumaker, MS 500-201	1
Attention: R. L. Cummings, MS 500-201	1
Attention: C. K. Swartz, MS 500-201	3 + 1 repro.
Attention: N. D. Sanders, MS 302-1	1
Attention: Dr. A. E. Potter, MS 302-1	3
Attention: C. S. Corcoran, MS 500-201	1

	No. of Copies
Attention: George Mandel, MS 5-1	2
Attention: Report Control Office	1
Attention: Technology Utilization Office, MS 3-16	1
National Aeronautics and Space Administration	
Langley Research Center	
Langley Station	
Hampton, Virginia 23365	
Attention: W. C. Hulton	1
Attention: E. Rind	1
Jet Propulsion Laboratory	
4800 Oak Grove Drive	
Pasadena, California 91103	
Attention: John V. Goldsmith	1
Attention: Don W. Ritchie	1
Institute for Defense Analysis	
Connecticut Avenue, N.W.	
Washington, D. C. 20546	
Attention: R. Hamilton	1
Advanced Research Projects Agency	
Department of Defense, Pentagon	
Washington, D. C. 20546	
Attention: Dr. C. Yost	1
Naval Research Laboratory	
Department of the Navy	
Washington, D. C. 20546	
Attention: E. Broncato, Code 6464	1
Attention: M. Wotaw, Code 5170	1
Attention: Dr. V. Linnenbom, Code 7450	1
Attention: Dr. C. Klick, Code 6440	1
U. S. Army Signal Research and Development Laboratory	
Fort Monmouth, New Jersey	
Attention: Power Sources Branch	1
Air Force Cambridge Research Center	
Air Research and Development Command	
United States Air Force	
Laurence G. Hanscom Field	
Bedford, Massachusetts	
Attention: Col. G. de Giacomo	1

	No. of Copies
Air Force Ballistic Missile Division	
Air Force Unit Post Office	
Los Angeles 45, California	
Attention: Col. L. Norman, SSEM	1
Attention: Lt. Col. G. Austin, SSZAS	1
Attention: Lt. Col. A. Bush, SSZME	1
Attention: Capt. A. Johnson, SSZDT	1
Attention: Capt. W. Hoover, SSTRE	1
Office of the Chief of Engineers	
Technical Development Branch	
Washington, D. C.	
Attention: James E. Melcoln/ENGMC-ED	1
Aeronautical Research Laboratories	
Office of Aerospace Research, USAF	
Wright-Patterson Air Force Base	
Dayton, Ohio	
Attention: Mr. D. C. Reynolds, ARX	
Chief, Solid State Physics, Research Lab.	1
Aeronautical Systems Division	
Air Force Systems Command	
United States Air Force	
Wright-Patterson Air Force Base, Ohio	
Attention: P. R. Betheand	1
Attention: Mrs. E. Tarrants/WWRNEM-1	1
Flight Vehicle Power Branch	
Air Force Aero Propulsion Laboratory	
Wright-Patterson Air Force Base, Ohio	
Attention: Joe Wise/Code APIP-2	1
Flight Accessories Aeronautics Systems Division	
Wright-Patterson Air Force Base	
Dayton, Ohio	
Attention: James L. Matice, ASRCN-22	1
Aerospace Corporation	
P. O. Box 95085	
Los Angeles 45, California	
Attention: Dr. G. Hove	1
Attention: Dr. F. Mozer	1
Attention: V. J. Porfune	1
Attention: Dr. I. Spiro	1
Attention: Technical Library Documents Group	1

	No. of Copies
Battelle Memorial Institute	
505 King Avenue	
Columbus, Ohio	
Attention: L. W. Aukerman	1
Attention: R. E. Bowman	1
Attention: T. Shielladay	1
Bell and Howell Research Center	
360 Sierre Madre Villa	
Pasadena, California	
Attention: Alan G. Richards	1
Bell Telephone Laboratories, Incorporated	
Murray Hill, New Jersey	
Attention: W. L. Brown	1
Attention: U. B. Thomas	1
Clevite Corporation	
Electronic Research Division	
540 East 105th Street	
Cleveland 8, Ohio	
Attention: Fred A. Shirland	1
Attention: Dr. Hans Jaffe	1
The Eagle-Picher Company	
Chemical and Material Division	
Miami Research Laboratories	
200 Ninth Avenue, N. E.	
Miami, Oklahoma	
Attention: John R. Musgrave	1
Energy Conversion, Incorporated	
336 Main Street	
Cambridge 42, Massachusetts	
Attention: G. J. McCaul	1
General Electric Company	
Electric Components Division	
316 East Nineth Street	
Owensboro, Kentucky	
Attention: F. D. Dyer, Jr.	1
Heliotek Corporation	
12500 Gladstone Avenue	
Sylmar, California	
Attention: Eugene Ralph	1

	No. of Copies
Hughes Aircraft Company Aerospace Group, R&D Division Culver City, California Attention: C. A. Escoffery	1
International Rectifier Corporation 239 Kansas Street El Segundo, California Attention: Irwin Rubin	1
Leesona Moos Laboratories 90-28 Van Wyck Expressway Jamaica 18, New York Attention: Stanley Wallack	1
Material Research Corporation Orangeburg, New York 10962 Attention: Vernon E. Adler	1
Martin Company Orlando, Florida Attention: W. A. Headley, Jr.	1
National Cash Register Company Physical Research Department Dayton 9, Ohio Attention: R. R. Chamberlin	1
North American Aviation, Incorporated Autonetics Division Anaheim, California Attention: R. R. August	1
Perkin-Elmer Company Optical Coating Section Norwalk, Connecticut Attention: Jim Beardsley	1
Philco Corporation Blue Bell, Pennsylvania Attention: Mr. A. E. Mace	1
RCA Laboratories Radio Corporation of America Princeton, New Jersey Attention: P. Rappaport	1

	No. of Copies
Sandia Corporation Albuquerque, New Mexico Attention: F. Smits	1
Sylvania Electronic Products, Incorporated Electron Tube Division Emporium, Pennsylvania Attention: Georgiana Larrabee, Librarian	1
Union Carbide Corporation Parma Research Center Technical Information Services P. O. Box 6116 Cleveland, Ohio 44101	1
Solid-State Electronics Laboratory Stanford Electronics Laboratories Stanford University Stanford, California Attention: Prof. G. L. Pearson	1
Westinghouse Electric Corporation Research and Development Laboratories Churchill Borough, Pennsylvania Attention: H. G. Chang	1
Westinghouse Electric Corporation Semiconductor Division Youngwood, Pennsylvania Attention: Don Gunther	1
Massachusetts Institute of Technology Security Records Office Room 14-0641 Cambridge 39, Massachusetts	1

Added

Lockheed Missiles & Space Company
Technical Information Center
3251 Hanover Street
Palo Alto, California